Universidade de Lisboa

Faculdade de Farmácia

PAMAM and PPI dendrimers as delivery systems of rose bengal to treat basal cell carcinoma: a photodynamic therapy preliminary approach

Ana Sofia Dias Martins

Mestrado Integrado em Ciências Farmacêuticas

2020

Universidade de Lisboa

Faculdade de Farmácia

PAMAM and PPI dendrimers as delivery systems of rose bengal to treat basal cell carcinoma: a photodynamic therapy preliminary approach

Ana Sofia Dias Martins

Monografia de Mestrado Integrado em Ciências Farmacêuticas apresentada à Universidade de Lisboa através da Faculdade de Farmácia

Orientador: Professora Catedrática, Barbara Klajnert-Maculewicz

Co-orientador: Professora Auxiliar, Ana Catarina Beco Pinto Reis

2020

University of Łódź - Poland

Faculty of Biology and Environmental Protection

PAMAM and PPI dendrimers as delivery systems of rose bengal to treat basal cell carcinoma: a photodynamic therapy preliminary approach

Ana Sofia Dias Martins

ERASMUS+ Traineeship Programme

Supervisor: Full Professor, Barbara Klajnert-Maculewicz

Co-supervisor: Assistant Professor, Ana Catarina Beco Pinto Reis

2020

ABSTRACT

Basal cell carcinoma (BCC) is the most diagnosed skin cancer worldwide. Despite growing slowly and rarely metastasize, BCC can lead to gross disfigurement of the tumor region. As the main site for tumors is the head and neck, it is very common that patients remain with unpleasant cosmetic outcomes.

Currently, surgery is the standard treatment of BCC. However, surgery is not applicable to all clinical situations. Photodynamic therapy (PDT) arises as a promising management option for low-risk BCC in the cases in which surgery is not feasible. PDT presents excellent cosmetic outcomes. Side-effects are few and generally well-tolerated. PDT is a minimally invasive procedure. However, PDT possesses some drawbacks, mainly related to the photosensitizers (PSs) used, such as high tendency to aggregate, possible toxicity, low cellular uptake and poor selectivity. In order to overcome those issues, dendrimers emerge as a possible solution. Dendrimers are promising delivery systems that could be useful to improve PSs' detrimental characteristics.

In this master thesis, we have developed complexes of rose bengal (RB), a PS, and several dendrimers: polyamidoamine (PAMAM) G3, PAMAM G4, polypropylenimine (PPI) G3 and PPI G4. The efficiency of the four types of dendrimers to form complexes with RB was studied resorting to spectrofluorimetric studies and zeta potential measurements. To investigate whether the photodynamic behavior of RB was maintained after the complexation with dendrimers, singlet oxygen ($^1O_2$) production assay and cytotoxicity studies were performed.

Concerning the obtained results, a satisfactory molar ratio for all complexes was achieved, regardless of the type and generation of dendrimers. $^1O_2$ production assay demonstrated that even when grafted on dendrimers, RB was able to keep its photodynamic properties. Moreover, G3 complexes produced more $^1O_2$ than free RB. Likewise, MTT assay revealed that RB behavior was not influenced by dendrimers as complexes showed similar cytotoxicity as free RB. Therefore, dendrimers revealed to have potential as delivery systems of PSs with application in PDT.

Keywords: basal cell carcinoma, photodynamic therapy, dendrimers, rose bengal.

RESUMO

O carcinoma basocelular (BCC) é o cancro de pele mais diagnosticado em todo o mundo. Apesar de crescer lentamente e raramente metastizar, o BCC pode provocar desfiguração grave na região do tumor. Como a principal zona em que aparecem os tumores é na região da cabeça e pescoço, é muito comum que os doentes permaneçam com lesões inestéticas.

A cirurgia é a primeira linha de tratamento do BCC. Contudo, esta estratégia não é aplicável a todos os casos clínicos. A terapia fotodinâmica (PDT) surge como uma opção de tratamento promissora para os tumores de baixo risco nos casos em que a cirurgia é impraticável. A PDT apresenta excelentes resultados estéticos. As reações adversas são poucas e geralmente bem toleradas. Trata-se de um procedimento minimamente invasivo. No entanto, a PDT apresenta algumas desvantagens, principalmente relacionadas com os fotossensibilizadores (PSs) usados, tais como elevada tendência de agregação, possível toxicidade, baixa internalização celular e fraca seletividade. De forma a contornar estes problemas, surgem os dendrímeros. Os dendrímeros são sistemas de transporte promissores que podem ser úteis para melhorar as características prejudiciais dos PSs.

Esta dissertação de mestrado propõe-se a desenvolver complexos de rosa bengala (RB), um PS, com vários dendrímeros: poliamidoamina (PAMAM) G3, PAMAM G4, polipropilenimina (PPI) G3 e PPI G4. A eficiência dos quatro tipos de dendrímeros em formar complexos com a RB foi estudada recorrendo a estudos espetrofluorimétricos e à análise do potencial zeta. Para investigar se a atividade fotodinâmica da RB se mantinha após a complexação, foi realizado o ensaio de produção do singleto de oxigénio ($^1O_2$) e estudos de citotoxicidade.

Relativamente aos resultados, foi obtida uma razão molar satisfatória para todos os complexos, independentemente do tipo e da geração dos dendrímeros. O ensaio de produção de $^1O_2$ demonstrou que mesmo ligada aos dendrímeros, a RB manteve a sua atividade fotodinâmica. Além disso, os complexos com dendrímeros G3 produziram mais $^1O_2$ que a RB. Da mesma forma, o ensaio de MTT revelou que o comportamento da RB não foi influenciado pelos dendrímeros, pois os complexos mostraram ter uma citotoxicidade semelhante à da RB. Assim, os dendrímeros revelam ter potencial como sistemas de transportes de PSs com aplicação na PDT.

Palavras-chave: carcinoma basocelular, terapia fotodinâmica, dendrímeros, rosa bengala.

ACKNOWLEDGMENTS

First, I want to thank Professor Barbara Klajnert-Maculewicz for accepting me as her ERASMUS student and for giving me this exciting research project. I want to express thanks to Professor Anna Janaszewska, Krzysztof Sztandera, M.Sc., and Dr. Michal Gorzkiewicz as well. They guided me through this project and had taught me a lot about doing research while I was at Faculty of Biology and Environmental Protection in Łódź. I would also want to thank Professor Catarina Reis for introducing me Professor Barbara's research work and for making the contact that took me to Poland, where I had the best experience of my life so far. In addition, I want to thank her for continuing to be my supervisor as she has been for more than a year by now.

A thank you to my friends, Alexandra Sousa and Maria João Quitério, who were my laboratory partners at Faculty of Pharmacy, and, in some way, continued to do so even when we were working in different laboratories. I want to express thanks for their friendship and understanding as they also know how it feels like failing many times and the happiness of a good result.

An acknowledgement is also needed to my hometown friends, Alexandra Melo, Angela Rodrigues, Flávia Luzío, Julieta Diogo, Pilar Faustino and Rita Carvalho, for their friendship and support in all aspects of life.

Lastly, the most important thank you is for my family and Pedro, my boyfriend, for their support through all this journey and for believing in me even when I don't.

CONTENTS

LIST OF FIGURES

LIST OF TABLES

ABBREVIATIONS

- **ABDA** - 9,10-antherachenediyl-bis(methylene) dimalonic acid
- **ALA** - Aminolevulinic Acid
- **BCC** – Basal Cell Carcinoma
- **Dend-RB complexes** – Dendrimers-Rose Bengal complexes
- **DMSO** - Dimethyl sulfoxide
- **DPBS** - Dulbecco's phosphate buffered saline
- **EPR** - Enhanced Permeability and Retention
- **G** - Generation
- **HEPES** - 4- (2-hydroxyethyl) -1-piperazineethanesulfonic acid)
- **HPI** - Hedgehog Pathway Inhibitors
- **MAL** – Methylaminolevulinate
- **MTT** - 3- (4, 5- dimethylthiazol-2-yl) -2, 5-diphenyltetrazolium bromide
- **MW** – Molecular Weight
- **NPs** – Nanoparticles
- $^{1}O_{2}$ – Singlet Oxygen
- **PAMAM** – Polyamidoamine
- **PBS** - Phosphate Buffered Saline
- **PDT** - Photodynamic Therapy
- **PLL** - Poly-L-lysine
- **PPI** – Polypropylenimine
- **PS** – Photosensitizer
- **RB** – Rose Bengal
- **ROS** – Reactive Oxygen Species
- **sBCC** – superficial BCC
- **SD** – Standard Deviation
- **USA** – United States of America
- **UV** – Ultraviolet

1. INTRODUCTION

1. 1. Cancer

Cancer is a complex genetic disease in which several mutations are required for creating abnormal cells that divide without control. This unruled multiplication leads to tissue disorganization, heterogeneous cell populations and malignancy (1). According to GLOBOCAN 2018 statistics, there were about 18.1 million new cancer cases and 9.6 million cancer deaths worldwide in 2018. An interesting finding is that Europe accounts for nearly a quarter (24.1%) of the total cancer cases; however, it only represents 9% of the global population. In addition, cancer is the first or second leading death cause in 91 of 172 countries. Therefore, it can be seen as a public health issue (2).

Cancer etiology includes both intrinsic and non-intrinsic factors. Intrinsic factors refer to errors that happen in cell division and cause DNA mutations, in the absence of non-intrinsic factors, whilst non-intrinsic factors are all the other factors. Non-intrinsic factors can be endogenous (inflammation, hormones, growth factors, reactive oxygen species (ROS), etc.) or exogenous (for example tobacco, viruses or drugs) (3). So, the risk factors individuals can avoid are related to non-intrinsic factors, especially exogenous ones (4).

1.2. Basal Cell Carcinoma

Basal cell carcinoma (BCC) is the most common skin cancer worldwide and it is increasingly incident and prevalent (5). However, as cancer registries do not collect data on BCC, these indexes are difficult to estimate (6). Nonetheless, American Cancer Society predicts that there are more than 2 million new cases per year in the United States of America (USA) (7) and some studies foresee that the incidence worldwide is rising 4% to 8% annually (8–10).

Despite being so prevalent, BCC grows slowly and rarely metastasizes (< 0.1%) (11). BCC is a commonly nonaggressive cancer but it can destroy cartilage, bone and other tissues and disfigure the region where the tumor lies. As the main site for lesions is the head and neck (80%), patients may remain with unpleasant cosmetic outcomes (12).

Aging, genetic predisposition, immunosuppression and being Caucasian, especially with light eyes and hair, are risk factors for developing BCC. However, ultraviolet (UV) radiation exposure is the most important risk factor to consider (13). UV radiation, especially UVB, contributes directly to BCC pathogenesis by inducing mutations in tumor suppressor genes (14). Another known pathogenesis mechanism of BCC is the dysregulation of the hedgehog

pathway, a signaling pathway that is essential for proper cell proliferation and tissue regeneration (15). Additionally, some rare genetic syndromes, such as Gorlin syndrome and Xeroderma pigmentosum, are linked to BCC pathogenesis (16).

Regarding BCC diagnosis, the lesions are inspected with naked eye examination and/or dermatoscopy to search for indicative characteristics of basal cell tumors. Biopsy is the standard method to diagnose BCC and it is also useful to select the most suitable treatment (7).

1.3. Available therapeutics for BCC

Currently, there are multiple approaches for BCC management and the treatment of choice depends on the size, shape and consequently, the risk of the tumor, whether it is recurrent and/or metastatic and lesion location (11).

In the majority of cases, complete surgical excision (including Mohs surgery) is the treatment of choice due to its high cure rate. Nevertheless, surgery is not applicable to all tumors (16). Therefore, nonsurgical options are available. With regards to the low-risk BCCs, destructive methods, topical therapies or photodynamic therapy (PDT) can be selected, whereas radiotherapy and hedgehog pathway inhibitors (HPI) are alternatives to advanced tumors (17). **Figure 1** schematizes BCC management options.

Destructive methods include curettage alone or followed by electrodesiccation and liquid nitrogen cryotherapy. In order to use those techniques, patients must be carefully selected (18). As protocols for these methods are not standardized, procedures are difficult to compare and cure rates are difficult to evaluate. Some studies show that recurrence rates 5 years after treatment for curettage and cryotherapy are 3% to 19% and 8% to 40%, respectively (19,20). So, destructive methods are not routinely performed (18).

Concerning topical therapies, 5-fluorouracil was the first topical drug approved to treat BCC (17), but its use was largely replaced by imiquimod, a toll-like receptor 7 (TLR-7) agonist that induces T-cells mediated apoptosis of cancer cells (7). Additionally, ingenol mebutate is an off-label option for the treatment of BCC (17). Ingenol mebutate was firstly approved to treat actinic keratosis and while it is still possible to prescribe it in the USA, its marketing license was suspended by the European Medicines Agency due to the possible increase of skin cancers, including BCC (21).

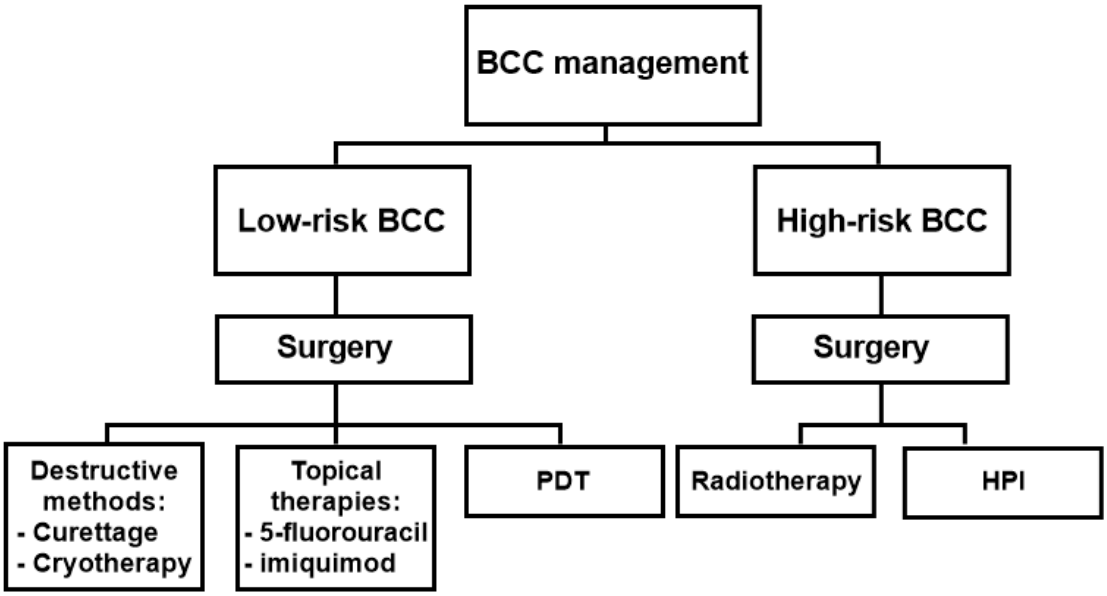

Figure 1 – Schematization of BCC management options.

PDT is also an alternative for low-risk BCC patients. This approach is based on the topical or systemic administration of a photosensitizer (PS) that induces toxicity after irradiation with a specific wavelength of visible light in the presence of oxygen. **Figure 2** schematizes the PDT mechanism. When a PS absorbs an adequate quantum energy, the electron in the outermost molecular orbital is excited to the first singlet excited state, recognized as being highly unstable (22). Therefore, this electron needs to waste the surplus of energy. The excited PS can accomplish that loss by fluorescence emission, internal conversion (heat production) or intersystem crossing, in which a more stable excited state is reached, the triplet state. PDT mechanism relies on the formation of that triplet state (23,24). As the triplet excited PS is a more long-lasting molecular specimen than the one on the singlet state, it has time to transfer energy to other molecules via two different pathways. In the type I pathway, the PS transfers an electron to other molecules, creating free radicals and ROS. The type II mechanism is based on the direct transfer of energy from the triplet state PS to molecular oxygen, generating a singlet oxygen ($^1O_2$) and the PS returns to its ground state (25). $^1O_2$ is a powerful oxidizer that induces oxidative damage to biomolecules, leading to its malfunctioning and consequently, to cell death (26). Type II pathway is of the most importance in PDT as most PSs operate through this mechanism (23).

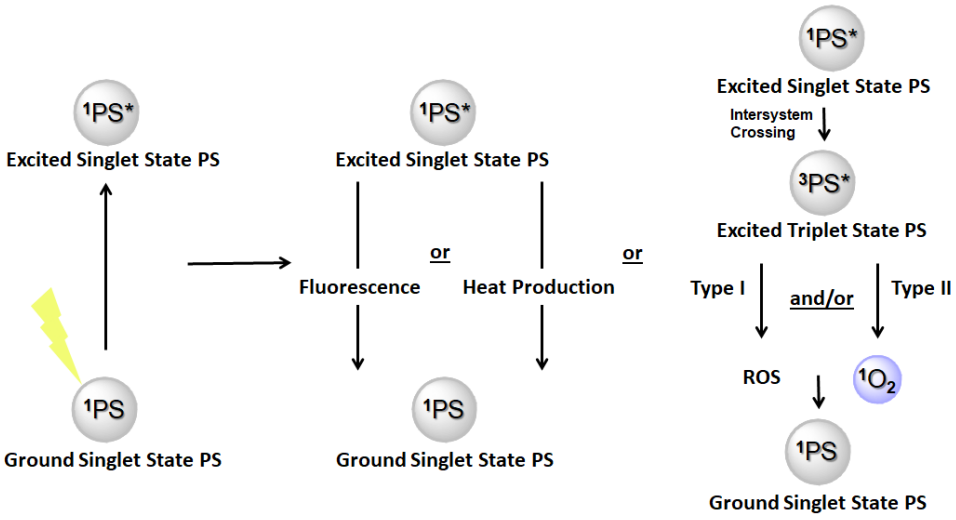

Figure 2 – Schematic illustration of the PDT mechanism.

PDT presents important advantages over other treatment options, including excellent cosmetic outcomes and application to large and multiple lesions. It is a less invasive procedure and possesses well-tolerated side effects, being the most common itching and a burning sensation while irradiation occurs (27). Additionally, due to the PDT principle, as only tumor areas are irradiated, even when PS enters non-cancer cells they will not be affected as they are not exposed to illumination (28). All the same, the ROS created cannot harm adjacent healthy cells because these oxygen noxious species have a brief lifespan (10 - 320 μs) and a short distance of migration within cells (10 – 55 nm) (25).

Literature review shows that superficial BCC (sBCC) are the most responsive to PDT with cure rates ranging from 72 to 100%. Aminolevulinic acid (ALA) and methylaminolevulinate (MAL) are the two approved PSs to use in BCC treatment. When comparing its effectiveness with other topical therapies for sBCC, a 3-year follow-up randomized controlled trial revealed that imiquimod is superior and 5-fluorouracil is not inferior to MAL-PDT. However, MAL-PDT is superior to imiquimod in elderly patients (29).

In contrast to the previous alternatives to surgical excision, radiation therapy and HPI inhibitors (vismodegib and sonidegib) are chosen for advanced and metastatic BCCs. Radiotherapy is an effective procedure as it presents low recurrence rates (around 8%) (7). Regarding HPI inhibitors, while complete responses are not highly obtained (30%), 73% of patients experienced partial improvements such as tumor shrinkage (30). As stated above, these two alternatives are just considered when no other is possible, as they are indicated for high-risk cases and also have the heavier side effects (18).

1.4. Nanotechnology

The interest in using nanotechnology to deliver drugs, especially anticancer agents, has been rising in recent years. Nanotechnology uses selected materials to produce nanoscale particles sized between 1 and 100 nm (31). The nano size together with a high surface-to-volume ratio promotes a different and beneficial behavior of these nanocarriers, when compared with large sized particles (32).

Nanoparticles (NPs) have the ability of modifying the pharmacokinetics of drugs. NPs might improve drugs' absorption, especially the low-water-solubility ones, because the most commonly used materials are hydrophilic and NPs' high surface-volume ratio increases cellular uptake (33). Biodistribution and metabolism can be also changed, as NPs improve the selectivity of actives and consequently, reduce their side effects. In the particular case of solid cancers, the targeting effect might happen due to the enhanced permeability and retention (EPR) phenomenon (32). The EPR effect was first mentioned by Matsumura and Maeda in 1986 (34). This effect is based on the fact that NPs will accumulate easily in tumors because of their disorganized and poor structured vasculature and also because their blood vessels are very prone to leakage as epithelium tight junctions are absent or non-functional. Moreover, lymphatic drainage is underdeveloped (35). Additionally, NPs might diminish drug metabolism and increase its half-life in circulation. These remarkable characteristics of NPs turn them into a highly desired strategy to deliver drugs (33).

Hence, there are some developments in this field for BCC management. To date, many nanocarriers have been used to try to obtain a more efficacious therapy for BCC such as liposomes (36,37), transfersomes (38), polymeric NPs (32) and dendrimers (24), as was studied in this master thesis.

1.5. Dendrimers

Originally synthesized by Tomalia *et al*. in 1985 (39), dendrimers or "starburst polymers" were first described as a marvel of chemical synthesis. Nowadays, these nanocarriers are one of the most attractive options for diseases' diagnostic and treatment (40).

Dendrimers are tree-shaped, highly branched symmetrical macromolecules with three well-defined structural regions (**Figure 3**): a central core, which is covalently linked to multiple branching units (the number of layers determines the dendrimer generation - G), and terminal groups that provide the interesting multifunctional surface of dendrimers (41). These surface moieties can be useful for creating complexes with drugs either by covalent, electrostatic or

hydrophobic bonds. Complexes can also be formed through encapsulation of the drug inside dendrimers' internal cavities (42).

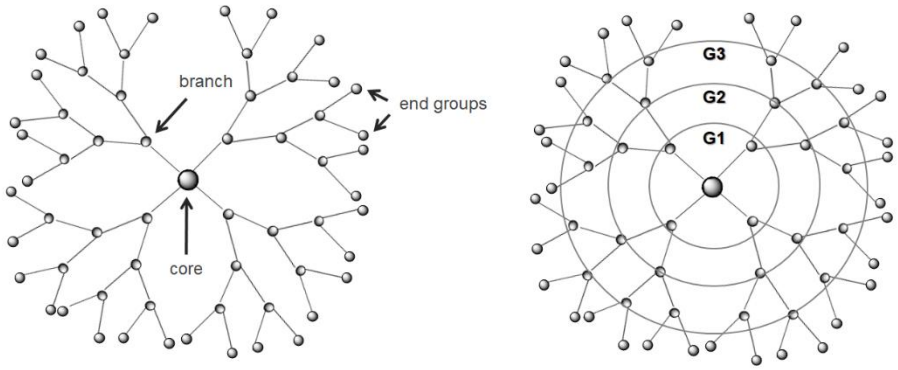

Figure 3 – Schematic representation of dendrimers' structure.

The unique structure of dendrimers can be obtained by the convergent and the divergent synthesis methods (**Figure 4**). In the convergent growth, dendritic fragments (dendrons) are synthesized individually and then linked to a polyfunctional molecule, which turns into the dendrimer core. Due to steric hindrance that occurs when one tries to bound bulky groups to a smaller molecule, this method is preferred for low-generation dendrimers (43). Hence, the size difference between intermediate products and the final molecule makes the purification step easier and faster. Concerning the divergent method, dendrimers grow each time that monomers' layers are sequentially added, first to the central core and then to the other layers, increasing dendrimer's layers and consequently, its generation. The latter method is used to build larger dendrimers. The preparation of a greater structure implies that branches' defects are more common and as the dendrimer's structure is constructed gradually, purification is a time-consuming process (42). Besides these two major synthetic routes, there are other possible approaches such as hypercores, branched monomers, double-exponential growth, lego and click chemistry (41).

As referred earlier, nanotechnology is thriving due to the attractive characteristics of nanomaterials. Dendrimers possess the aforementioned advantageous properties and also distinguish positively from traditional polymers because of their unmatched structure. Unlike other polymers, dendrimers have an enormous advantage: a low polydispersity index. The uniform dendrimers' populations are obtained thanks to the well-controlled polymerization (44). Monodispersity is utterly required to achieve reproducibility (45). In addition, dendrimers possess a large number of end-groups that can be easily functionalized in order to attach a high number of actives or change physicochemical and pharmacokinetic properties (44).

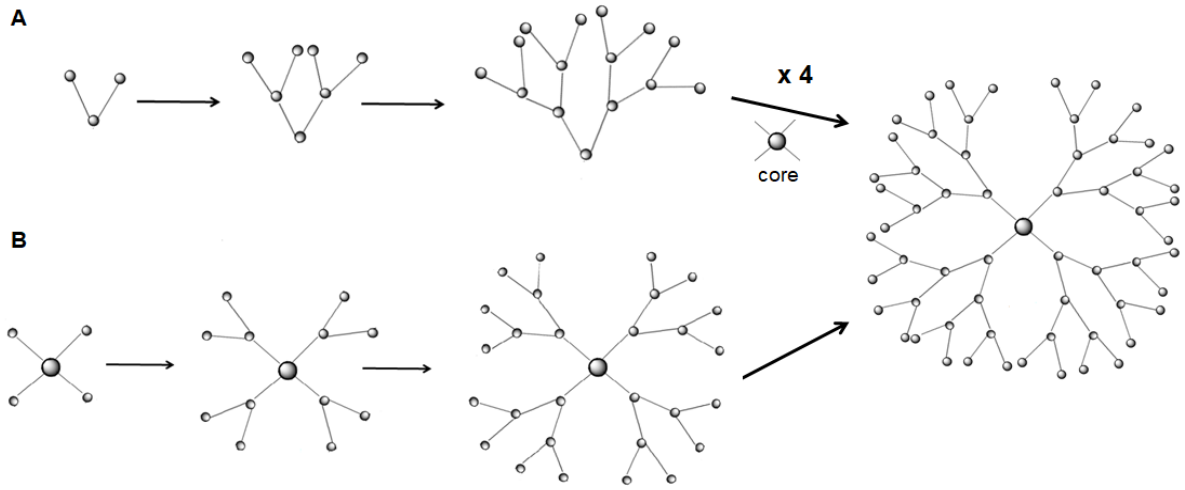

Figure 4 – Schematic representation of convergent (A) and divergent (B) synthesis methods.

Finally, the so-called 'dendritic effect' is worth mentioning (**Figure 5**). The 'dendritic effect' includes the 'multivalency effect' or the efficacy absence of the monomers in contrast to the situation when the same monomers are assembled in a dendrimer, and the 'generation effect' or the properties modification, either positive or negative, when dendrimer's generation increases. The former effect is more connected to the less-known application of dendrimers, being drugs by themselves (46).

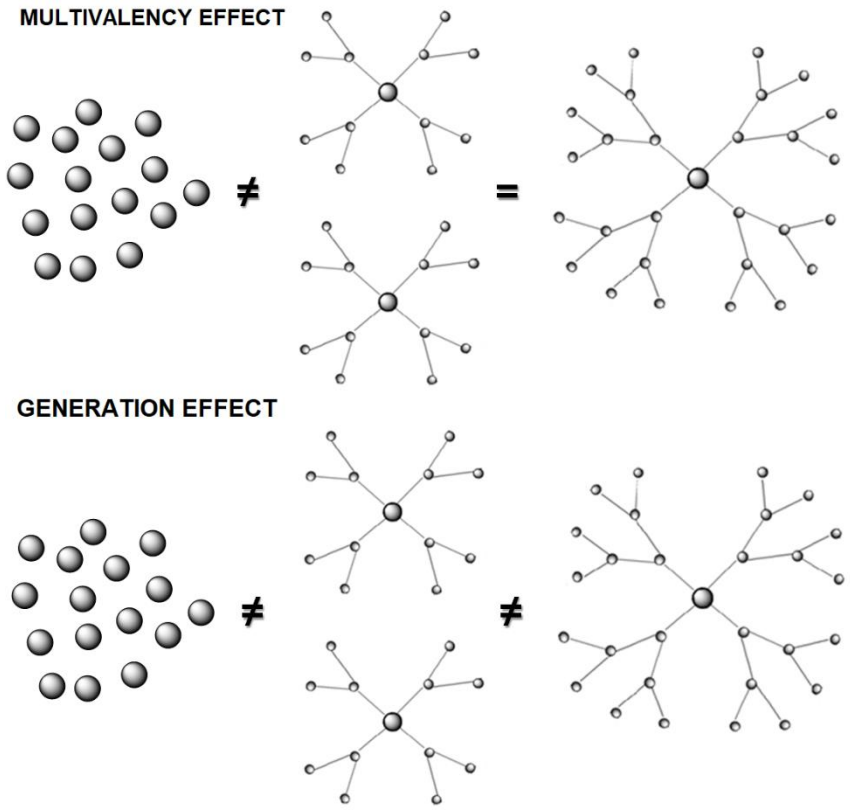

Figure 5 – The 'dendritic effect'. Adapted from Caminade *et al*., 2014 (46).

Dendrimers are not just an efficient system for drug and gene delivery or even innovative contrast agents, they are also characterized with antimicrobial activity against a wide range of bacteria, yeast (*Candida albicans*) and viruses. VivaGel® - developed by Starpharma - is the first approved product in which dendrimers are drugs *per se*. In an initial phase, VivaGel® was introduced in condoms to prevent sexually transmitted infections, such as HSV-2, HPV and HIV. Now, it is also used to prevent and treat bacterial vaginosis (47,48).

The main drawback associated to dendrimers, especially the positively-charged ones, is their potential cytotoxicity. Not only has the surface charge influence toxicity, but also the concentration, generation or even the chemistry of the core of the dendrimer (49). Cationic macromolecules strongly interact with the negatively-charged phospholipids that constitute cell membranes, destabilizing them and provoking lysis. Many attempts have been tried to reduce this effect. The functionalization of the end-groups with polyethylene glycol (PEG), the so-called PEGylation, is the most common strategy (42).

Dendrimers are not just one type of polymer but actually a wide class of nanoscopic molecules. To date, many dendrimers were synthetized. Polyamidoamine (PAMAM), polypropylenimine (PPI) and poly-L-lysine (PLL) are the most commonly used dendrimers in nanomedical applications (50). As PAMAM and PPI dendrimers (**Figure 6**) were the ones used in this experimental work, their characteristics will be further assessed. Regarding the similarities, both PAMAM and PPI dendrimers' surface groups are primary amine groups with

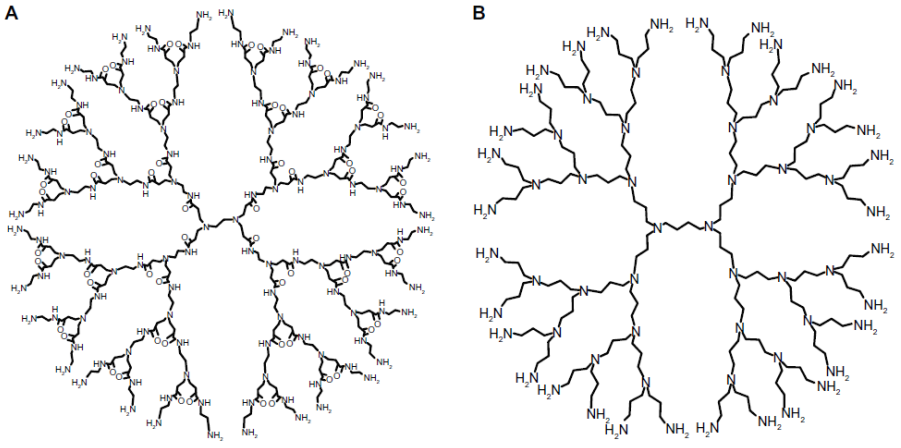

Figure 6 – PAMAM G3 (A) and PPI G3 (B) dendrimers. Extracted from Shao *et al.*, 2011 (51).

a pKa of about 10.0, therefore the end-groups are protonated in aqueous environments, conferring excellent water solubility to these macromolecules (51). However, PPI dendrimers are more hydrophobic than PAMAM dendrimers as the interior is composed of tertiary amines and alkyl chains and the external layer has higher density of surface groups. In addition, PPI

dendrimers (of the same generation) are generally smaller. PAMAM dendrimers' branching units count seven bonds, whereas PPI dendrimers have only three (52). In respect of the toxicity issue, as both dendrimers are cationic molecules, they display some cytotoxicity. While some authors refer that the toxicity of PAMAM and PPI dendrimers is equivalent (52,53), a study indicates that PPI dendrimers are 50-fold more toxic than PAMAM dendrimers on MCF-7 and A549 cells (51).

1.6. Our preliminary approach for BCC treatment

Considering the high BCC prevalence, the management of this skin malignancy implies significant healthcare costs. Apalla *et al*. review showcased that non-melanoma skin cancers (BCC and squamous cell carcinoma) total healthcare costs are already very high. In 2010, Australia spent $511 million and annually, the USA expends around $650 million (54). Thus, it is necessary to find more cost-effective treatments in order to alleviate healthcare systems burden. Additionally, the main site for lesions is the head and neck, so strategies that combine cost-effectiveness and good cosmetic outcomes are extremely required (12). PDT seems to be this so-wanted BCC management option. PDT is a long-term efficacious treatment (55), offers excellent cosmetic outcomes (28) and studies suggest that PDT is a cost-effective therapy (28,56). Caekelbergh *et al.* economic evaluation indicates that MAL-PDT has better value for money than surgical excision, especially in sBCC cases (56). Nevertheless, PDT presents some drawbacks, mainly related to the PSs such as PS's unwanted dark toxicity, instability, hydrophobicity, poor selectivity and cellular uptake (57,58). These disadvantages must be surpassed in order to become an even more attractive treatment. In this project, we used nanotechnology (dendrimers) to overcome these challenges. Rose bengal (RB) was the PS of choice in this PDT approach. The photodynamic effects of RB are mediated via the type II pathway of ROS generation (59). Its molecular structure is shown in **Figure 7**. The interesting applicability of RB in the biomedical field drove attention to this anionic and hydrophilic purplish-red dye (60). At first, RB was employed in the ophthalmological clinical practice as a conjunctival stain to investigate dry eye pathologies. Nowadays, it has been replaced by other dyes, such as lissamine green, due to the ocular discomfort felt when RB enters into the cells. This effect is probably caused by its photodynamic properties. As RB is a PS, it is able to produce ROS when exposed to light, causing cellular stress and discomfort (61).

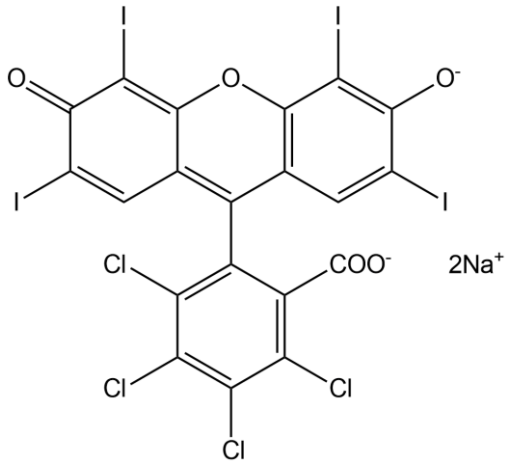

Figure 7 – Molecular structure of RB.

Thus, our aims were to prepare complexes of RB and four types of dendrimers (PAMAM G3, PAMAM G4, PPI G3 and PPI G4), understand the complexation efficiency and evaluate the photodynamic behavior of RB when complexed with PAMAM and PPI dendrimers. To achieve those aims, the methodologies used were spectrofluorimetric studies, zeta potential measurements, $^1O_2$ production assay and cytotoxicity (MTT) studies. The ultimate goal is to use this renewed PDT approach to treat BCC.

2. MATERIALS AND METHODS

2.1. MATERIALS

PPI G4 (32 terminal amino groups and molecular weight (MW) of 3514 g/mol) and G5 (64 terminal amino groups and MW of 7168 g/mol) were purchased from SyMO-Chem (Eindhoven, Netherlands). In order to follow the uniform nomenclature for polyamide dendrimers (62), in this report PPI G4 will be referred as PPI G3 and PPI G5 as PPI G4. PAMAM G3 (32 terminal amino groups and MW of 6909 g/mol) and G4 (64 terminal amino groups and MW of 14215 g/mol), RB, fetal bovine serum, penicillin/streptomycin solution, trypsin-EDTA solution, 9,10 - antherachenediyl-bis(methylene) dimalonic acid (ABDA) probe and 3-(4, 5-dimethylthiazol-2-yl)-2, 5-diphenyltetrazolium bromide (MTT) were obtained from Sigma-Aldrich (St. Louis, MO, USA). 154 CF culture medium and calcium chloride were purchased from Gibco (ThermoFisher Scientific, MA, USA) and trypan blue from Invitrogen (ThermoFisher Scientific, MA, USA). Dulbecco's phosphate buffered saline (DPBS) without calcium or magnesium was obtained from Biowest (Riverside, MO, USA). DMSO (dimethyl sulfoxide) was purchased from POCH (Gliwice, Poland). Murine basal cell carcinoma cell lines (AsZ, BsZ and CsZ) were kindly provided by Dr. Ervin Epstein (Children's Oakland Research Institute, Oakland, CA, USA). All other reagents were of analytical grade.

2.2. METHODS

2.2.1. Preparation of complexes

In order to obtain RB complexes, the first step was to prepare stock solutions of RB (10 mM) and dendrimers (1 mM). RB was dissolved in PBS (10 mM, pH 7.4). PAMAM dendrimers were dissolved in PBS. PPI dendrimers were dissolved in water. RB stock solution was kept in the fridge and was protected from light. Dendrimers stock solutions were kept in the freezer. Then, stock solutions were diluted in HEPES (10 mM, pH 7.4) to produce new solutions in the desired concentration, in order to prepare complexes with different molar ratios. Lastly, dendrimers solutions were added to RB solution and then mixed until a homogeneous solution was achieved.

Throughout this master thesis, the complexes formed between RB and PAMAM G4 will be referred as PAMAM G4:RB complexes and the same nomenclature will be followed for the other three complexes composed by the other three dendrimers: PAMAM G3:RB, PPI G4:RB and PPI G4:RB complexes. When in need to reference all complexes, the used terminology will be 'Dend-RB complexes'.

2.2.2. Characterization of the Dend-RB complexes and interaction of RB and the different dendrimers

Spectrofluorimetric studies

Spectrofluorimetric studies were performed to assess the interaction of RB and the different dendrimers with the aim of finding complexes' molar ratio. Fluorescence emission spectra were obtained with a LS 55 fluorescence spectrometer (PerkinElmer, MA, USA) at a temperature of 37ºC. All samples were prepared in HEPES buffer (10mM, pH 7.4) and placed in quartz cells, being continuously stirred along the experiment. The excitation wavelength was set to 525 nm and spectra were recorded between 540 and 650 nm. It was observed that dendrimers alone do not emit fluorescence in this wavelength range. The slit width for excitation and emission monochromators was 5 and 7.5 nm, respectively. A RB solution at a constant concentration of 1 µM was titrated with a dendrimer solution in concentrations ranging from 0.02 µM to 1 µM, in order to maintain the molar ratio of Dend-RB complexes between 1:50 to 1:1.

Zeta potential measurements

Zeta potential measurements were performed using electrophoretic mobility technique in Zetasizer Nano ZS (Malvern Instruments, Malvern, UK) at a constant temperature of 25ºC. All samples were prepared in HEPES buffer (10 mM, pH 7.4). The complexes with RB and the different dendrimers were separately characterized. A constant concentration (10 µM) of dendrimer solution was placed in DTS 1070 folded capillary cells and titrated with concentrations of RB solution ranging from 10 µM to 500 µM, which corresponds to 1:1 to 1:50 Dend-RB complexes molar ratio.

2.2.3. Assessment of the RB photodynamic activity after complexation using singlet oxygen production assay

ABDA, at a concentration of 5 µM, was the chosen probe to evaluate the $^1O_2$ production by free RB, Dend-RB complexes and free dendrimers. The molar ratio of all Dend-RB complexes was 1:10. The samples of RB and Dend-RB complexes were prepared at a 0.125, 0.25, 0.5, 0.75 and 1 µM concentration of RB. Dendrimers were prepared at a concentration of 0.1 µM. All samples were prepared in HEPES buffer (10mM, pH 7.4). After samples' preparation, 100 µL of each solution was transferred to a 96-well black plate. Negative control wells were filled with 100 µL of HEPES buffer. All measurements were registered with Fluoroskan Ascent FL microplate reader (ThermoFisher Scientific, MA, USA). The excitation wavelength was set to 355 nm and the emission wavelength to 460 nm. The plates were shaken before every measurement. The first measurement was performed without ABDA to

check if samples emit fluorescence in this region. None of the samples revealed that behavior. Then, the probe was added to each well and a measurement of ABDA fluorescence without irradiation was recorded (t=0 min). Following this first measurement, the plate was placed 20 cm under the Q. Light Pro Unit lamp (Q. Light, Rorschach, Switzerland), which was equipped with a filter (Q. Light, Rorschach, Switzerland) that emits visible light from 385 to 780 nm. The plate was irradiated for 25 minutes and the measurement of ABDA fluorescence emission was recorded every 5 minutes (from 5 to 30 min). The slopes of the fluorescence emission curves were considered to compare the $^1O_2$ production between samples. $^1O_2$ generation (%) was defined as relative to the negative control wells.

2.2.4. Assessment of the RB photodynamic activity after complexation using cytotoxicity studies

Cell Culture

Murine basal cell carcinoma cell lines (AsZ, BsZ and CsZ) were kept in 154 CF culture medium supplemented with 5% penicillin/streptomycin, 0.05 mM calcium and 2% chelexed, heat-inactivated fetal bovine serum. The cells were maintained in T-75 culture flasks at 37ºC with a 5% CO_2 atmosphere and checked every 2 to 3 days. When a confluence of 80 – 90% was reached, cell subculture was performed. The cells were harvested with a solution of 0.25% (w/v) of trypsin and 0.03% (w/v) of EDTA.

Trypan blue exclusion method

In order to determine the number of viable cells, the method of trypan blue exclusion was employed. 10µL of cells suspension was mixed with 10µL of trypan blue staining solution. This mixture was placed in a Countess Cell Counting Chamber Slide (ThermoFisher Scientific, MA, USA). The slide was introduced in a Countess Automated Cell Counter (ThermoFisher Scientific, MA, USA) and then, the instrument counted the cells.

MTT Assay

The cell viability of AsZ, BsZ and CsZ cell lines after the incubation with RB, Dend-RB complexes and free dendrimers was evaluated by MTT assay. MTT assay is based on the reduction of a yellow water-soluble salt by the succinate dehydrogenase in the mitochondria of metabolically active cells into a water-insoluble purple crystal, formazan. This insoluble product can be measured spectrophotometrically upon solubilization in an organic solvent, such as DMSO (63).

The cells were seeded in 96-well plates at a concentration of 3.0×10^4 cells/well and incubated for 24h. After that time, the culture medium was removed from the wells and 100 µL

of sample was added to each well. The samples of RB and Dend-RB complexes were prepared at a 0.25, 0.5, 1 and 2 μM concentration of RB. Free dendrimers were prepared at a concentration of 0.2 μM. The molar ratio of all Dend-RB complexes was 1:10. All samples were prepared in culture medium. Culture medium was used as the negative control. After 5h of cells' incubation with samples, the medium was removed and replaced with DPBS. In order to assess the cytotoxic effect after illumination, half of the prepared plates were irradiated with a Q. Light Pro Unit lamp (Q. Light, Rorschach, Switzerland) equipped with the same filter used in the $^1O_2$ production assay. After 30 minutes of irradiation, DPBS was removed, replaced by fresh medium and the plates were incubated for 24h. The other half of the plates were used to assess the 'dark toxicity' so, after being washed with DPBS, the wells were filled with culture medium and incubated for 24h. Following the incubation time, the wells were washed with DPBS and 50 μL of MTT reagent (0.5 mg/mL) was added to each well and the plates were incubated for 3h. Then, MTT reagent was removed and 100 μL of DMSO was added to each well to dissolve the formazan crystals. The absorbance was measured at 570 nm in a PowerWave HT Microplate Spectrophotometer (BioTek, Winooski, VT, USA). Cell viability (%) was presented as percentage of untreated wells.

2.2.5. Statistical Analysis

Each value is presented with a mean value ± standard deviation (SD). The statistical differences were evaluated with analysis of variance (ANOVA). Statistical analysis was conducted in GraphPad Prism Version 6 (GraphPad Software, San Diego, CA, USA) and the differences were deemed significant at a $p<0.05$.

3. RESULTS

3.1. Characterization of the Dend-RB complexes and interaction of RB and the different dendrimers

Spectrofluorimetric studies

The aim of the spectrofluorimetric studies was to find the optimal molar ratio of the complexes formed between RB and two types of dendrimers of different generations: PAMAM and PPI, both G3 and G4. This analytical technique was possible to employ due to the RB ability of emitting fluorescence (57). According to the literature, dendrimers can show strong fluorescence emission (64,65). Due to this concern, it was verified that the dendrimers used in this study do not emit fluorescence at this wavelength range (data not shown). RB spectrum and spectra obtained in the study of the molar ratio of PPI G3:RB complexes are shown in **Figure 8**. Similar spectra were obtained for the other complexes with different dendrimers.

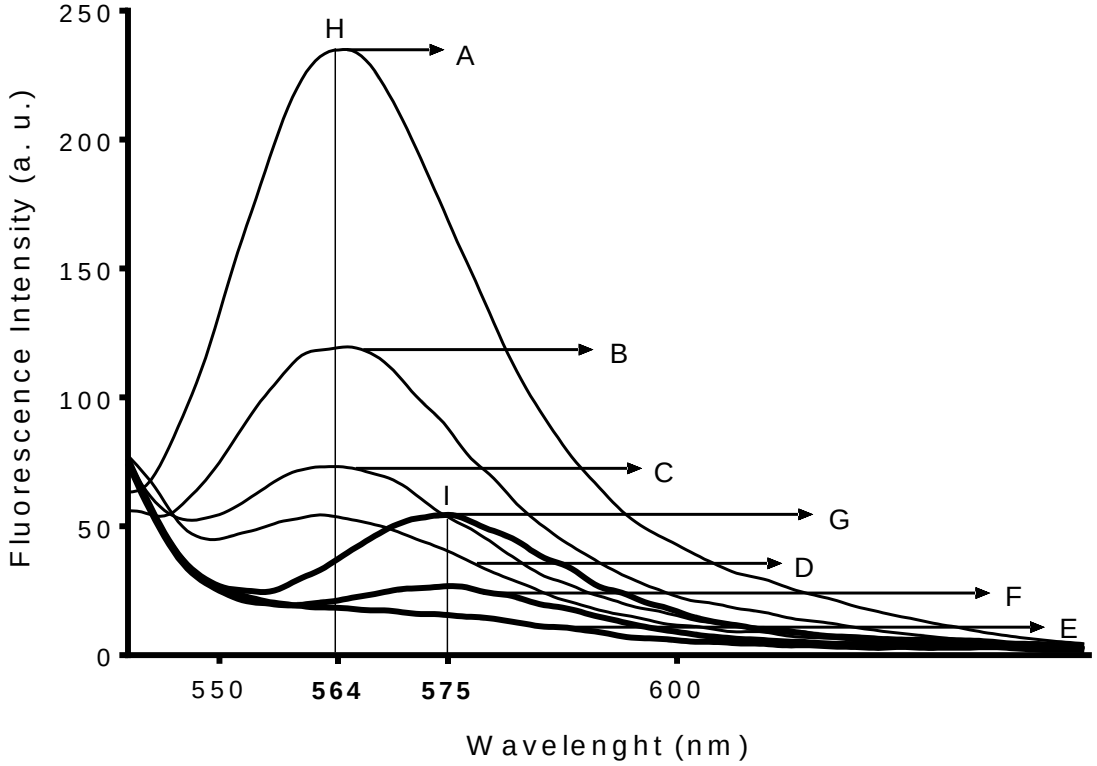

Figure 8 – Fluorescence spectrum of 1 µM RB (A) and spectra of PPI G3:RB at 1:50 (B), 1:40 (C), 1:35 (D), 1:20 (E), 1:5 (F) and 1:1 (G) molar ratio. The peak of RB fluorescence (H) was verified at λ = 564 nm and the peak of the shift (I) at λ = 575 nm.

For all complexes, we started the spectrofluorimetric study by assessing the fluorescence spectrum of 1 µM RB (Figure 8 – A), which presented a maximum peak of fluorescence at 564

nm (Figure 8 – H). Next, we added 0.02 µM of dendrimer (1:50 Dend-RB molar ratio). Following this titration, the quenching of RB fluorescence was observed (Figure 8 – B). Considering PPI G3:RB complexes as example, the quenching phenomenon (Figure 8 – B, C and D) was verified from 1:50 to 1:25 molar ratio. Then, at 1:20 molar ratio (Figure 8 – E), a shift of the peak was noticed. The red shift dislocated the maximum peak from 564 nm to 575 nm (Figure 8 – I). Finally, from 1:20 to 1:1 molar ratio (Figure 8 – E, F and G), the fluorescence intensity increased each time dendrimer's solution was added.

The values of fluorescence intensity at 564 nm and 575 nm of each molar ratio were used (F_{564}/F_{575}) to determine the maximum efficiency of dendrimers to complex with RB. The binding stoichiometry of complexes is indicated by the intersection of the curves. For PAMAM G3:RB, the molar ratio was 1:20 (Figure 9 – A), for PAMAM G4:RB it was 1:35 (Figure 9 – B), for PPI G3:RB it was 1:25 (Figure 9 – C) and for PPI G4:RB it was 1:35 (Figure 9 – D).

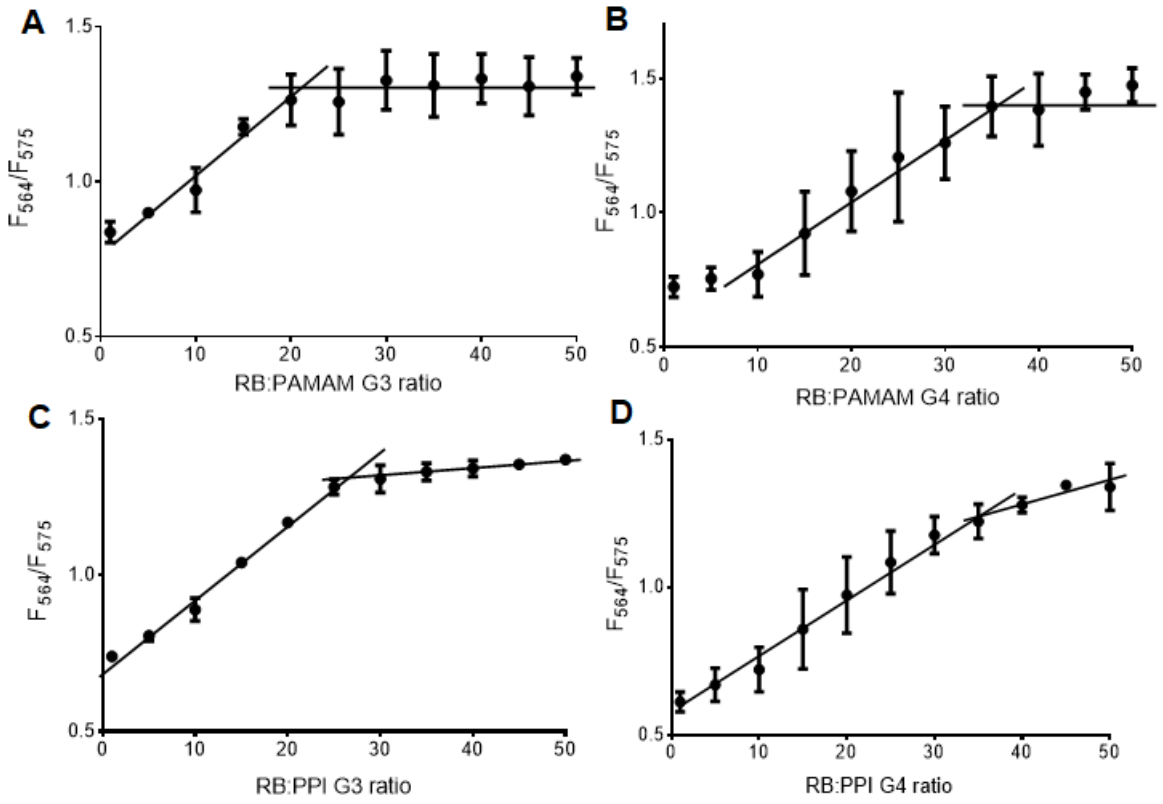

Figure 9 – Molar ratio determination of PAMAM G3:RB (A), PAMAM G4:RB (B), PPI G3:RB (C) and PPI G4:B (D) complexes. The results are presented as mean value ± SD.

Zeta Potential Measurements

Similarly to spectrofluorimetric studies, a titration with zeta potential measurements was performed. A 10 µM solution of dendrimer was titrated with crescent concentrations of RB. Zeta potential was registered and a titration curve for PAMAM G3:RB (Figure 10 – A), PAMAM G4:RB (Figure 10 – B), PPI G3:RB (Figure 10 – C) and PPI G4:RB (Figure 10 – D) complexes

was obtained. The titration curves allowed the evaluation of the molar ratio of complexes and the acquaintance of complexes' surface charge.

Regarding the molar ratio determination of complexes, for PAMAM G3:RB, the ratio was 1:20, for PAMAM G4:RB, 1:25, for PPI G3:RB, 1:20 and for PPI G4:RB, 1:30.

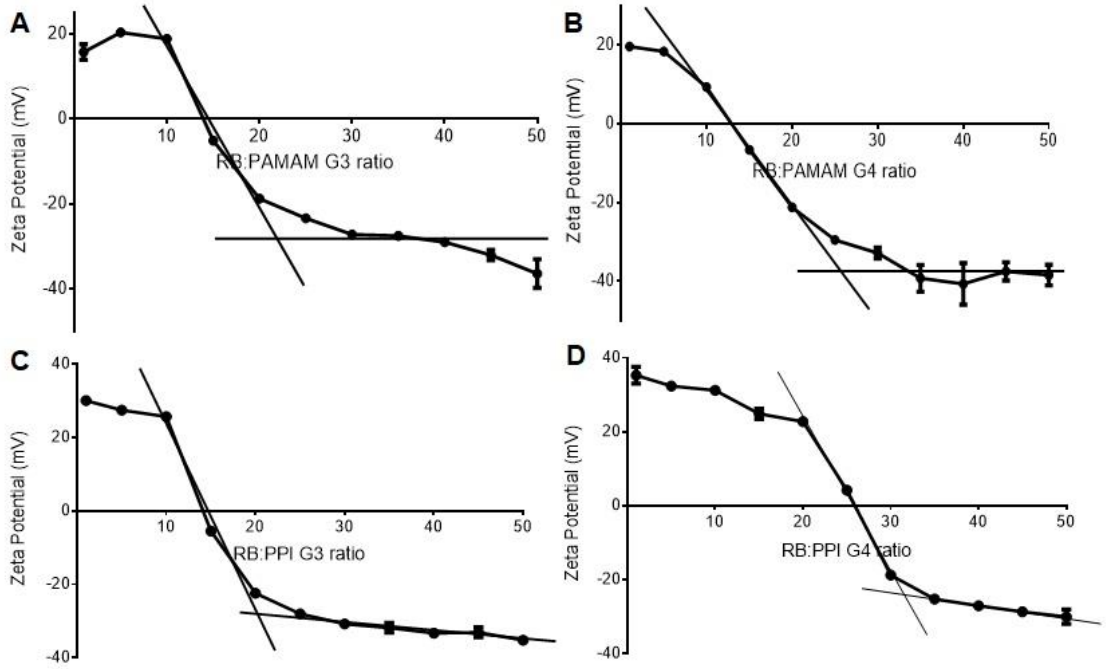

Figure 10 – Molar ratio determination of PAMAM G3:RB (A), PAMAM G4:RB (B), PPI G3:RB (C) and PPI G4:B (D) complexes through analysis of zeta potential titration curves. The results are expressed as mean value ± SD.

At 1:10 molar ratio, all complexes present positive surface charge. For the following studies in this report, the chosen complexes' molar ratio was 1:10. According to literature, several studies suggest that positively charged NPs are more efficiently internalized by cells than the anionic ones (66–69).

3.2. Assessment of the RB photodynamic activity after complexation using singlet oxygen production assay

As stated earlier, RB is a PS. Therefore, it induces the production of ROS when it absorbs light of a specific wavelength (61). One of the objectives of this report was to understand the photodynamic behavior of RB when complexed with dendrimers. Thus, the ability of this type II PS to generate $^1O_2$, even when complexed with the dendrimers in study, was assessed. In order to perform the $^1O_2$ production assay, a $^1O_2$ probe, ABDA, was used. Complexes' $^1O_2$ generation curves were compared with the $^1O_2$ generation curve of free RB (**Figure 11**). Both G4 complexes revealed to produce similar amounts of $^1O_2$ at all ranges of RB concentrations,

when compared with free RB. PAMAM G3:RB complexes induced higher production of $^1O_2$ at higher RB concentrations (0.75 and 1 µM). Regarding PPI G3:RB, complexes with 0.5 µM, 0.75 µM and 1µM of RB generated significantly more $^1O_2$ than free RB at the same concentration. Free dendrimers, at the highest concentration used in the complexes' production (0.1 µM), did not produce more $^1O_2$ than the negative control (**Figure 12**).

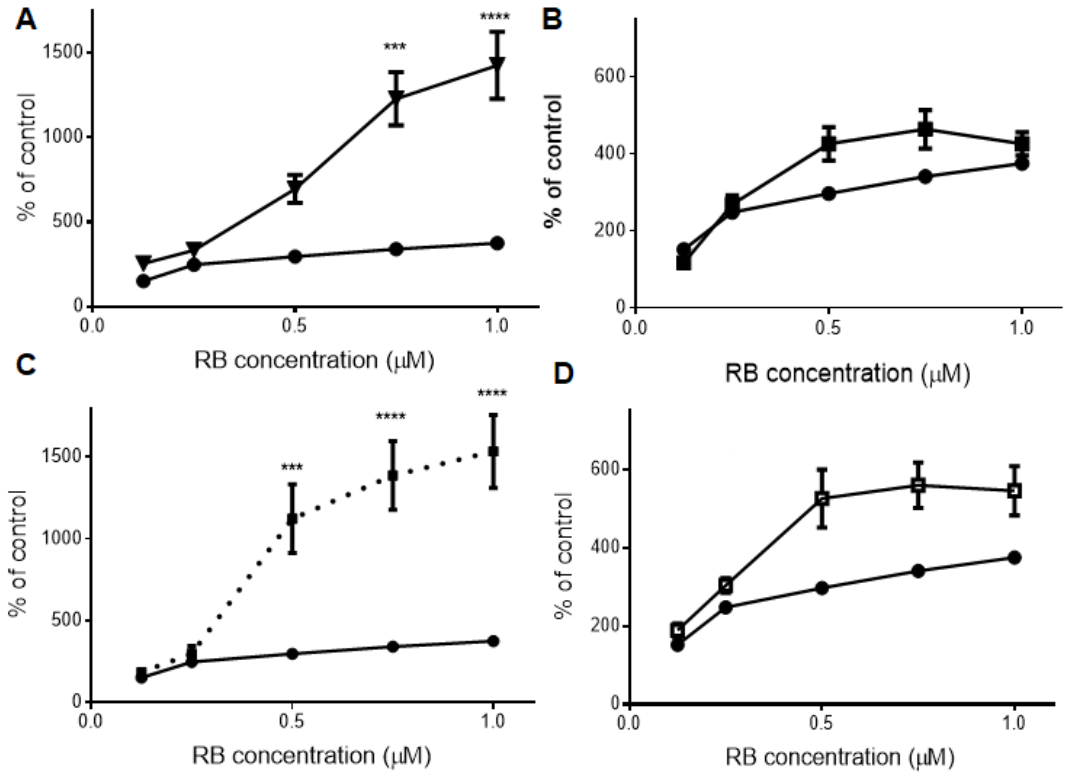

Figure 11 – $^1O_2$ generation of free RB (●), PAMAM G3:RB (▼), PAMAM G4:RB (■), PPI G3:RB (dotted line) and PPI G4:RB (□) complexes. The results are expressed as mean value ± SD. (*** p<0.001; ****p<0.0001).

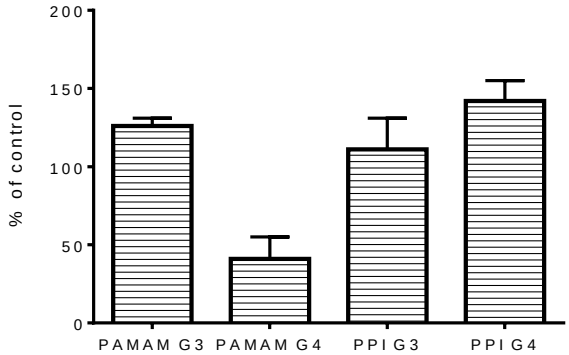

Figure 12 – $^1O_2$ generation of free dendrimers at 0.1 µM concentration.

3.3. Assessment of the RB photodynamic activity after complexation using cytotoxicity studies

Cells were viable accordingly to the trypan blue exclusion method and in a sufficient number to perform the cytotoxicity study. The cytotoxicity of complexes, free RB and free dendrimers was evaluated by MTT assay. MTT assay was conducted in AsZ, BsZ and CsZ cell lines. **Figure 13** depicts the results of MTT assay, presented as % of cell viability. The results displayed that the cytotoxicity of complexes was similar to the toxic action showed by free RB. In AsZ cell line, the reduction of cell viability was about 50%. Regarding BsZ cell line, the diminishment was around 70% and in CsZ cell line, 35%. However, in the CsZ cell line, PPI complexes did not follow the cytotoxicity behavior of RB. 'Dark toxicity' was also evaluated (**Figure 14**). Neither free RB nor complexes significantly decreased cell viability. The only exception was PAMAM G4:RB complexes, which slightly diminished cell viability of BsZ cell line at 1µM and 2µM RB concentration. However, the cell viability remained above 89%. Free dendrimers' cytotoxicity was also assessed with and without illumination and no cytotoxic effect was observed (data not shown).

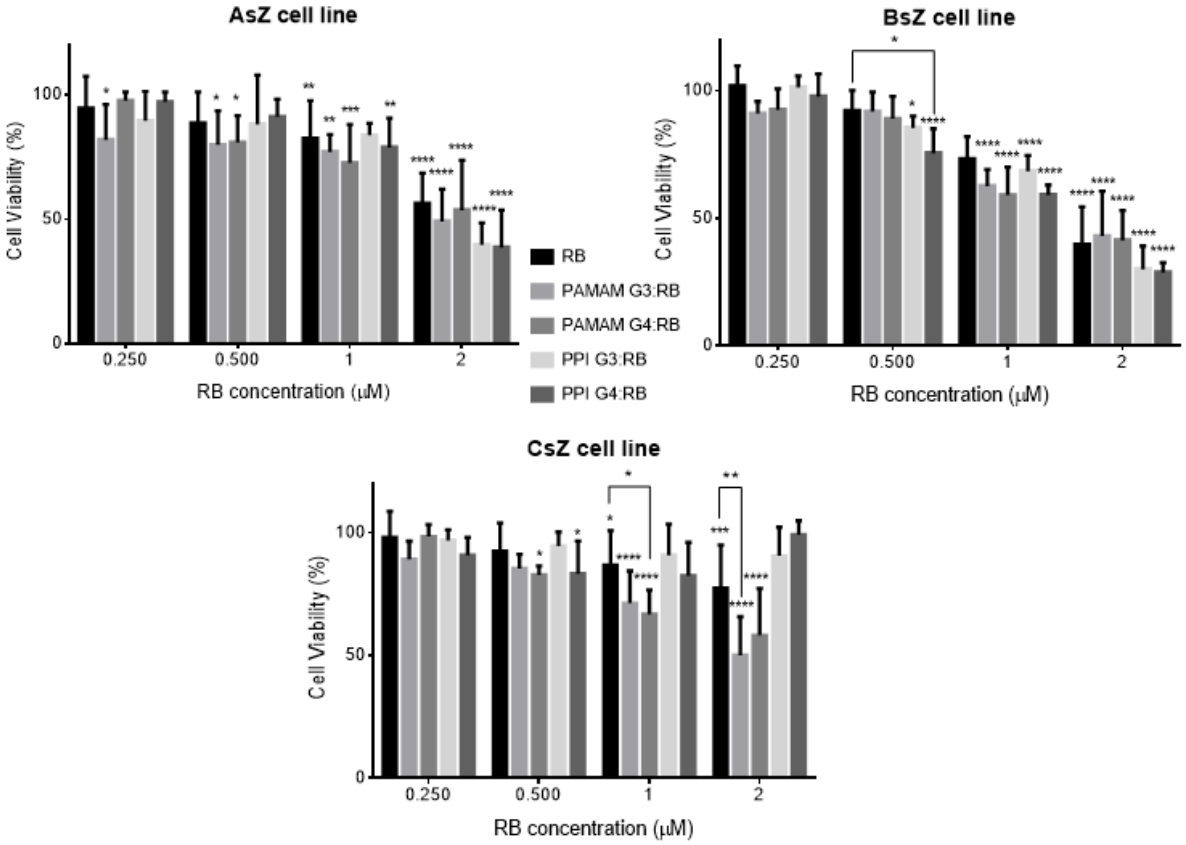

Figure 13 – AsZ, BsZ and CsZ cell viability (%) after 5h exposure to 0.25, 0.5, 1 and 2 µM of free RB, PAMAM G3:RB, PAMAM G4:RB, PPI G3:RB and PPI G4:RB complexes followed by 30 min of irradiation. The results are expressed as the mean value and the respective SD. (* p<0.05;** p<0.01;*** p<0.001;**** p<0.0001).

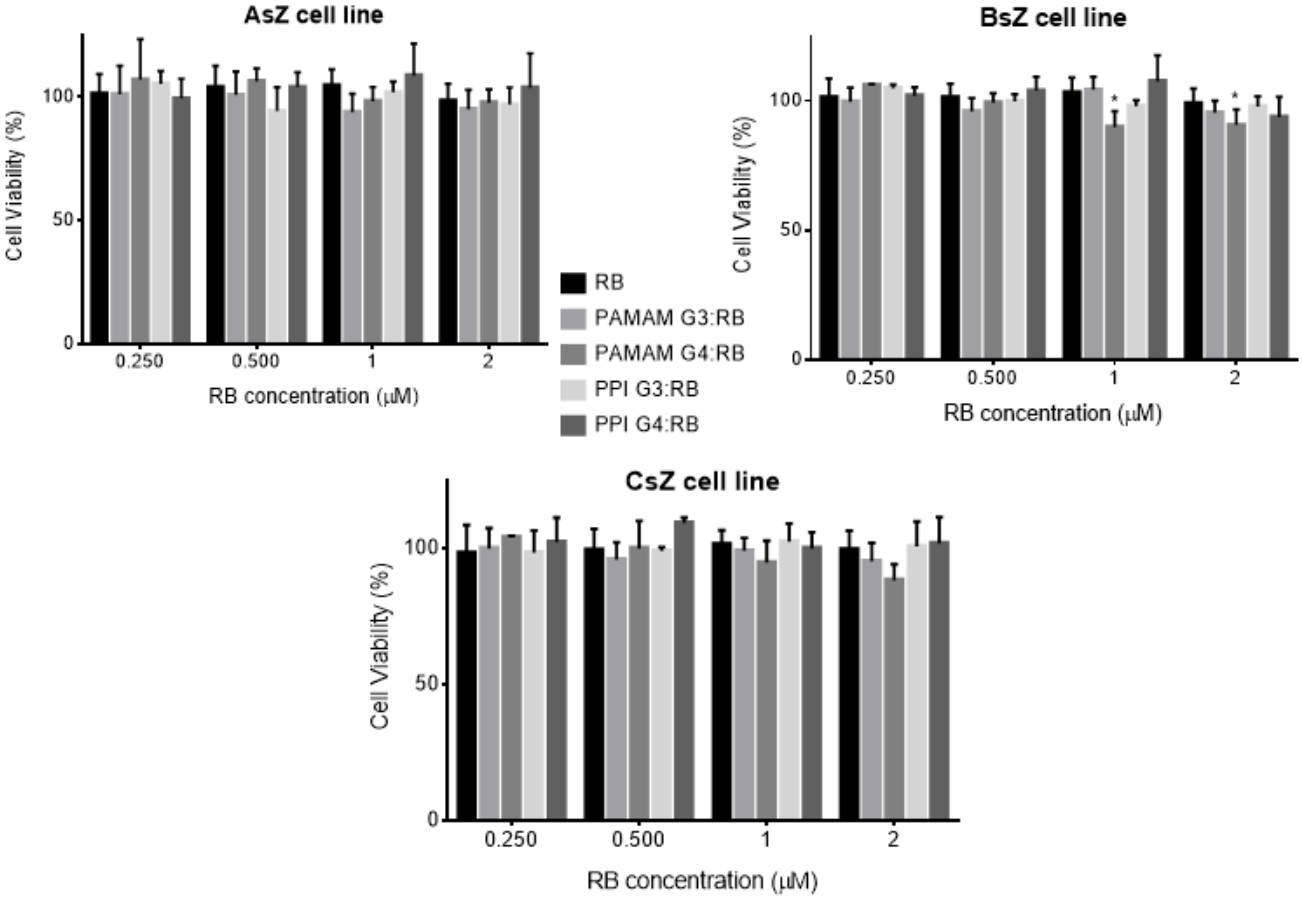

Figure 14 – AsZ, BsZ and CsZ cell viability (%) after 5h exposure to 0.25, 0.5, 1 and 2 μM of free RB, PAMAM G3:RB, PAMAM G4:RB, PPI G3:RB and PPI G4:RB complexes without irradiation. The results are expressed as the mean value and the respective SD. (* $p<0.05$).

4. DISCUSSION

As previously described, BCC is the most diagnosed skin cancer worldwide. PDT is a promising therapy for BCC (70). In fact, PDT is an approved treatment option for BCC tumors (71). However, some limitations related to the PSs' nature limits PDT application. High tendency to aggregate in aqueous environment, low cellular uptake and poor selectivity are some concerns about PSs. Nanotechnology could be useful to tackle those disadvantages (70). In this master thesis, the chosen nanocarriers were dendrimers. As PS, the model chosen was RB. This selection was supported in early research, which emphasized that phosphorus dendrimers could successfully form non-covalent complexes with PSs such as RB and methylene blue (57,58,72,73). As stated earlier, this experimental work focused on the complexation of negatively charged RB with four different cationic dendrimers – PAMAM G3 and G4 and PPI G3 and G4 – to check whether generation and type of dendrimer influences the complexation efficiency and the photodynamic behavior of RB.

Complexes' stoichiometry was assessed by spectrofluorimetric studies (**Figure 9**) and zeta potential titration (**Figure 10**). **Table 1** summarizes the results obtained by those two methods.

Table 1 – Comparison of complexes' molar ratio findings obtained with spectrofluorimetric studies and zeta potential measurements.

	PAMAM G3:RB	**PAMAM G4:RB**	**PPI G3:RB**	**PPI G4:RB**
Spectrofluorimetric Studies	1:20	1:35	1:25	1:35
Zeta Potential Measurements	1:20	1:25	1:20	1:30

In addition to revealing the molar ratio of complexes, spectrofluorimetric studies also gave information about how RB interacts with dendrimers. Upon addition of dendrimer, the intensity of fluorescence immediately diminished (**Figure 8** – A → B). The quenching of fluorescence might happen due to the interaction of carboxyl group of RB with an amino terminated group of the dendrimer (74). Then, the titration had been continued and at some point, a shift to higher wavelengths (red shift) happened. According to previous studies, the appearance of a shift indicates that complexes were successfully formed (74–77). Moreover, a red shift suggests that the binding between RB and dendrimers can be attributed to ionic bonds rather than RB being encapsulated inside dendrimers' pockets (57,77). Interestingly, the fluorescence intensity rose after the observation of the shift (**Figure 8** – E → F → G). This could be caused by the formation of complexes. As RB interacts with dendrimers' end groups through

ionic bonds, RB molecules are no longer free in solution (77). Molecule rigidity favors fluorescence (78).

Both methods indicate that G4 dendrimers form complexes with more RB molecules than the G3 ones. Thus, a higher loading capacity could be linked to dendrimers' generation and not to the type of dendrimer, finding that is in contrast with previous work; according to Shao *et al.*, PPI dendrimers loaded less phenylbutazone than PAMAM dendrimers, both having 32 amino terminated groups (51). The higher loading capacity of G4 dendrimers may be due to the higher number of cationic end-groups (42). As spectrofluorimetric spectra indicates, the relationship between RB and these cationic nanocarriers is mediated through electrostatic forces. So, one could think that the more positively charged surface groups a dendrimer has, higher molar ratios could be achieved. While it may be true, it could be argued that the molar ratio does not seem to increase in a proportional manner with the generation. One explanation might be that as generation increases, the outer structure becomes sequentially bulkier and the internal cavities becomes too small that it is difficult for more molecules to graft on the dendrimer due to the steric hindrance (79). This illustrates the so-called 'de Gennes's dense packing limit', which is more pronounced from G7 (80).

Surface charge plays a pivotal role in the cellular uptake of NPs. Indeed, surface charge modification is a common strategy to enhance cellular uptake (67,81). As cell membranes present a negative charge, positively charged NPs are generally internalized by cells to a higher extent than negatively or neutrally charged ones (82). Besides molar ratio determination, zeta potential measurements allowed the assessment of complexes' surface charge. Results showed that all complexes present positive surface charge at 1:10 molar ratio (**Figure 10**). Therefore, 1:10 was the chosen molar ratio for the following experiments.

The ability of a type II PS to generate $^1O_2$ is the basic mechanism of the PDT. $^1O_2$ is a highly cytotoxic agent and thus, very effective at killing cells (75). $^1O_2$ production assay was performed to assess if RB maintained its photodynamic activity after being complexed with dendrimers. ABDA probe was used to evaluate the $^1O_2$ production. In the presence of $^1O_2$, ABDA reacts with it through a [4+2] – cycloaddition (**Figure 15**). $^1O_2$ returns to its ground state and as ABDA transforms into an endoperoxide, the probe loses its fluorescence properties and the quenching phenomenon is observed (83).

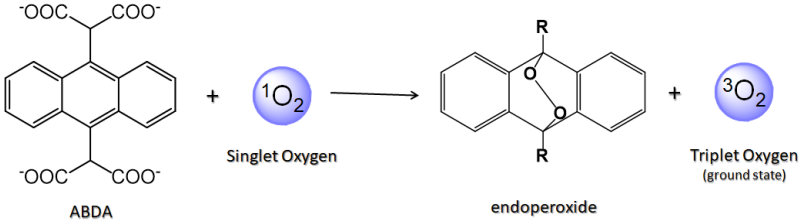

Figure 15 – ABDA reaction with $^1O_2$. Adapted from Entradas *et al.*, 2020 (83).

In the $^1O_2$ production assay, all complexes exhibited the ability to produce more $^1O_2$ than the control wells. In contrast with the findings of Kojima *et al*., none of the complexes showed to generate less $^1O_2$ than free RB (84). G4 complexes showed to yield similar $^1O_2$ quantity to free RB. However, complexes of RB with PAMAM G3 and with PPI G3 dendrimers produced significantly higher levels of $^1O_2$ (at higher RB concentrations) than free RB. Dabrzalska *et al*. also presented similar findings with complexes of RB and phosphorus G3 dendrimers (48 amino end groups) (72). The generation of a dendrimer is an utmost important property of these polymers (44). Here, we might be observing one more example of the aforementioned 'dendritic effect', more specifically the 'generation effect'. This interesting phenomenon might be happening because of what was mentioned earlier about the increase of surface density of the dendrimers that follows the dendrimer growth in generations. Higher generations have a more closed structure, therefore ligands have more difficulty to enter in the cavities or to bind to the surface terminal groups (85,86). So, the bond between RB and the amino end groups of a G3 dendrimer might be stronger and more stable than the same one with a G4 dendrimer. Hence, RB molecules are less prone to aggregate. Aggregates' formation, a major disadvantage of PSs, probably leads to self-quenching and decrease of the triplet state lifetime (87). Thus, a lower yield of $^1O_2$ is generated (88).

In vitro assays are a useful tool to preliminary assess the cytotoxic efficacy or safety of a given formulation (68). MTT assay was performed to determine the cytotoxicity of Dend-RB complexes, free RB and free dendrimers, both with and without irradiation. Herein, MTT assay was conducted in AsZ, BsZ and CsZ cell lines. Those three murine BCC cell lines are morphologically and genetically similar to BCC cells (89). An interesting finding was the nontoxic behavior of free dendrimers towards AsZ, BsZ and CsZ cell lines. Broadly speaking, cytotoxicity is the most mentioned disadvantage of dendrimers, especially of the cationic ones as are PAMAM and PPI dendrimers (90), however, it was not noticed in this experiment. Regarding the 'phototoxicity' results, complexes' cytotoxicity resembles the cell viability diminishment found for free RB. The only exception was observed for PPI:RB complexes towards CsZ cell line. At all ranges of concentration, cell viability remained above 85%. The G3 dendrimers ability to generate more $^1O_2$ in the $^1O_2$ production assay did not show the same behavior *in vitro*. Overall, RB showed that its photodynamic activity was kept even after the complexation with dendrimers. Dendrimers seem to be a suitable delivery system for RB (57,72); in a contrasting example, Kumar *et al.* study showed that gadolinium oxide coated dextran NPs displayed an inhibitory effect in regards to RB photodynamic efficacy (91). Additionally, the 'dark cytotoxicity' was assessed (**Figure 14**). The unwanted 'dark toxicity' is another main drawback of PSs (92). In previous studies, the decrease in cell viability prior to irradiation was reported (93,94). In our work, not only free RB induced no toxicity towards

cells that were in the non-irradiated plates, but also complexes showed that positive behavior. Only PAMAM G4:RB complexes demonstrated a slight diminishment in cell viability of the BsZ cell line. Nevertheless, cell viability remained above 89%. ISO 10993-5 considers that when cell viability remains above 80%, it indicates no cytotoxicity (95,96). Therefore, dendrimers seem to be a promising delivery system for PSs such as RB.

5. CONCLUSIONS

In this experimental work, we obtained complexes of RB with four dendrimers – PAMAM G3, PAMAM G4, PPI G3 and PPI G4 – with a satisfactory molar ratio for all. According to the results obtained, both spectrofluorimetric and zeta potential experiments were useful assays to predict complexes' molar ratio as these methods provided approximated results.

RB efficacy as a PS was maintained after complexation. This fact is very important considering the mechanism of cytotoxicity of PSs. In general, it relies on the production of ROS upon irradiation. Thus, it is utterly required that drug delivery systems do not eliminate the PS toxic effect. The $^1O_2$ production assay suggests that the complexation with dendrimers does not eliminate the ability of RB to generate $^1O_2$. In the same experiment, G3 dendrimers showed to significantly enhance the RB yield of $^1O_2$, which might lead to suppose that we could be observing a 'dendritic effect', the 'generation effect'. While G3 complexes showed that behavior in the $^1O_2$ production assay, this effect was not noticed in the MTT assay. However, cytotoxicity studies demonstrated once again that complexation did not affect RB photodynamic activity. The other important findings were that free dendrimers did not caused cytotoxicity and complexes were nontoxic without irradiation. Therefore, taken together, these results highlight that dendrimers seem to be promising nanocarriers of RB and possibly other PSs for PDT applications.

In the future, *in silico* studies could be interesting to perform in order to assess whether there is a difference between the strength of the bond formed between RB and G3 and G4 dendrimers. Additionally, it could help to better visualize their interaction. Flow cytometry is another appealing technique to test our complexes. It might be helpful to understand the extent of internalization of our complexes in AsZ, BsZ and CsZ cell lines. If the cellular uptake is not favorable, dendrimers' surface modification can be a strategy to improve that deficiency.

The added value of these fascinating polymers might lie in their ability to avoid the aggregation of RB. Thus, it could be interesting to investigate the capacity of Dend-RB complexes to stabilize RB and hinder aggregation. This could be assessed by performing long-term stability studies. Additionally, as dendrimers are drug delivery systems, these nanocarriers can possibly target the delivery of drugs towards cancerous tissues or, in our case, prevent the distribution of complexes to other tissues as the final formulation would be injected directly into the tumor. *In vivo* biodistribution studies are a useful tool to evaluate the behavior of Dend-RB complexes in a living organism. Thereby, a suitable animal model should be used, such as the immunocompetent Patched knockout mice.

6. REFERENCES

1. Vogelstein B, Kinzler TW. The multistep nature of cancer. Trends Genet. 1993;9(4):138–41.

2. Bray F, Ferlay J, Soerjomataram I. Global Cancer Statistics 2018 : GLOBOCAN Estimates of Incidence and Mortality Worldwide for 36 Cancers in 185 Countries. Ca Cancer J Clin. 2018;68(6):394–424.

3. Thompson P, Hannun YA. Evaluating intrinsic and non-intrinsic cancer risk factors. Nat Commun. 2018;9(1):1–12.

4. Lewandowska AM, Rudzki M, Rudzki S, Lewandowski T, Laskowska B. Environmental risk factors for cancer. Ann Agric Environ Med. 2019;26(1):1–7.

5. Berking C, Hauschild A, Kölbl O, Mast G, Gutzmer R. Basal Cell Carcinoma — Treatments for the Commonest Skin Cancer. Dtsch Arztebl Int. 2014;111(22):389–95.

6. Cordova M, Nehal KS, Rossi AM. Basal cell carcinoma: epidemiology, pathophysiology, clinical and histological subtypes, and disease associations. J Am Dermatology. 2019;80(2):303–17.

7. Marzuka AG, Book SE. Basal Cell Carcinoma: Pathogenesis, Epidemiology, Clinical Features, Diagnosis, Histopathology and Management. Yale J Biol Med. 2015;88(2):167–79.

8. Australian Institute of Health and Welfare. Cancer in Australia 2014: Actual incidence data from 1982 to 2011 and mortality data from 1982 to 2012 with projections to 2014. Asian-Pacific J Clin Oncol. 2015;11(3):208–20.

9. Rudolph C, Eisemann N. Incidence trends of nonmelanoma skin cancer in Germany from 1998 to 2010. J Ger Soc Dermatology. 2015;13(8):788–97.

10. Sng J, Om MM, Birm DK, Chia W, Med SM, Bee T, et al. Skin cancer trends among Asians living in Singapore from 1968 to 2006. J Am Dermatology. 2007;61(3):426–32.

11. Sreekantaswamy S, Endo J, Chen A, Butler D, Morrison L, Linos E, et al. Aging and the treatment of basal cell carcinoma. Clin Dermatol. 2020;37(4):373–8.

12. Bertozzi N, Simonacci F, Grieco MP, Grignaffini E. Single center evidence for the

treatment of basal cell carcinoma of the head and neck. Acta Biomed. 2019;90(1):77–82.

13. Peris K, Concetta M, Garbe C, Kaufmann R, Bastholt L, Basset N, et al. Diagnosis and treatment of basal cell carcinoma: European consensus e based interdisciplinary guidelines. Eur J Cancer. 2019;118:10–34.

14. Lewin JM, Carucci JA. Advances in the management of basal cell carcinoma. F1000Prime Rep. 2015;7(53):1–8.

15. Sobjanek M, Wo A, Lesiak A, Bednarski IA, W K. Alternative activation of hedgehog pathway induced by ultraviolet B radiation: preliminary study. Clin Exp Dermatol. 2018;43(5):518–24.

16. Migden MR, Lynn A, Chang S, Dirix L, Stratigos AJ, Lear JT. Emerging trends in the treatment of advanced basal cell carcinoma. Cancer Treat Rev. 2018;64:1–10.

17. Paoli J, Gyllencreutz JD, Fougelberg J, Backman EJ. Nonsurgical Options for the Treatment of Basal Cell Carcinoma. Dermatol Pract Concept. 2019;9(2):75–81.

18. Koelblinger P. New developments in the treatment of basal cell carcinoma: update on current and emerging treatment options with a focus on vismodegib. Onco Targets Ther. 2018;11:8327–40.

19. Rowe R, Sheskey P, Quinn M. Handbook of Pharmaceutical Excipients. Handb Pharm excipients, Sixth Ed. 2009;549–53.

20. Kuflik E. Cryosurgery for Skin Cancer: 30-Year Experience and Cure Rates. Dermatol Surg. 2004;30(2):297–300.

21. EMA suspends licence for ingenol mebutate (Picato). Drug Ther Bull. 2020;58(4):51.

22. Sztandera K, Marcinkowska M, Gorzkiewicz M, Janaszewska A, Laurent R, Zabłocka M, et al. In Search of a Phosphorus Dendrimer-Based Carrier of Rose Bengal: Tyramine Linker Limits Fluorescent and Phototoxic Properties of a Photosensitizer. Int J Mol Sci. 2020;21(12):4456.

23. Abrahamse H, Hamblin MR, Africa S, Hospital MG. New photosensitizers for photodynamic therapy. Biochem J. 2017;473(4):347–64.

24. Dabrzalska M, Janaszewska A, Zablocka M, Mignani S, Majoral JP, Klajnert-maculewicz B. Cationic Phosphorus Dendrimer Enhances Photodynamic Activity of Rose Bengal against Basal Cell Carcinoma Cell Lines. Mol Pharm. 2017;14:1821–30.

25. Mansoori B, Mohammadi A, Doustvandi MA, Kamari F, Gjerstorff MF, Baradaran B. Photodynamic therapy for cancer: role of natural products. Photodiagnosis Photodyn Ther. 2020;26:395–404.

26. Dogra V, Kim C. Singlet Oxygen Metabolism: From Genesis to Signaling. Front Plant Sci. 2020;10:1–9.

27. Fargnoli MC, Peris K. Photodynamic therapy for basal cell carcinoma. Futur Oncol. 2015;11:2991–6.

28. Savoia P, Deboli T, Previgliano A, Broganelli P. Usefulness of Photodynamic Therapy as a Possible Therapeutic Alternative in the Treatment of Basal Cell Carcinoma. Int J Mol Sci. 2015;16(10):23300–17.

29. Roozeboom MH, Arits AHMM, Mosterd K, Essers BAB, Rooij MJM De, Quaedvlieg JF, et al. Three year follow-up results of photodynamic therapy versus imiquimod versus fluorouracil for treatment of superficial basal cell carcinoma: a single blind, non-inferiority, randomized controlled trial. J Invest Dermatol. 2016;136(8):1568–74.

30. Group W, Bichakjian C, Armstrong A, Baum C, Iyengar V, Lober C, et al. Guidelines of care for the management of basal cell carcinoma. J Am Acad Dermatology. 2018;78(3):540–59.

31. Reis CP, Neufeld RJ. Nanoencapsulation I . Methods for preparation of drug-loaded polymeric nanoparticles. Nanomedicine Nanotechnology, Biol Med. 2006;2(1):8–21.

32. Dianzani C, Zara GP, Maina G, Pettazzoni P, Pizzimenti S, Rossi F, et al. Drug Delivery Nanoparticles in Skin Cancers. Biomed Res Int. 2014;1:1–13.

33. Montan X, Bajek A, Roszkowski K, Montorn JM, Giamberini M, Roszkowski S, et al. Encapsulation for Cancer Therapy. Molecules. 2020;25(1605):1–25.

34. Matsumura Y, Maeda H. A New Concept for Macromolecular Therapeutics in Cancer Chemotherapy : Mechanism of Tumoritropic Accumulation of Proteins and the Antitumor Agent Smancs1. Cancer Res. 1986;46(12):6387–92.

35. Golombek SK, May J, Theek B, Appold L. Tumor Targeting via EPR: Strategies to Enhance Patient Responses. Adv Dug Deliv Rev. 2018;130:17–38.

36. Natalia M, Febres-molina C, Esteban R, Zevallos-delgado C, Eugenia M, Paolino D, et al. Nanoformulation for potential topical delivery of Vismodegib in skin cancer treatment. Int J Pharm. 2019;565(5):108–22.

37. Cadinoiu AN, Rata DM, Atanase LI, Daraba OM, Gherghel D, Vochita G, et al. Aptamer-Functionalized Liposomes as a Potential Treatment for Basal Cell Carcinoma. Polymers (Basel). 2019;11(1515):1–17.

38. Fadel M, Samy N, Nasr M, Alyoussef AA. Topical colloidal indocyanine green-mediated photodynamic therapy for treatment of basal cell carcinoma for treatment of basal cell carcinoma. Pharm Dev Technol. 2017;22(4):545–50.

39. Polymers S, Oligomers S, Macromers T, Macromolecules D, Clusters O. A New Class of Polymers: Starburst-Dendritic Molecules. Polym J. 1985;17(1):117–32.

40. Majoral JP, Mignani SM, Shi X, Manuel J, Muñoz-fernández MÁ, Ceña V, et al. Dendrimers towards translational nanotherapeutics: Concise key step analysis. Bioconjug Chem. 2020;31(9):2060–71.

41. de Araújo RV, da Silva Santos S, Ferreira EI, Giarolla J. New advances in general biomedical applications of PAMAM dendrimers. Molecules. 2018;23(11):1–27.

42. Mendes LP, Pan J, Torchilin VP. Dendrimers as Nanocarriers for Nucleic Acid and Drug Delivery in Cancer Therapy. Molecules. 2017;22(1401):1–21.

43. Sandoval-Yanes C, Castro Rodriguez C. Dendrimers : Amazing Platforms for Bioactive Molecule Delivery Systems. Materials (Basel). 2020;13(570):1–20.

44. Dzmitruk V, Id EA, Ihnatsyeu-kachan A. Dendrimers Show Promise for siRNA and microRNA Therapeutics. Pharmaceutics. 2018;10(126):1–25.

45. Vega D La. Uniform polymer microspheres : monodispersity criteria , methods of formation and applications R eview. Nanomedicine. 2013;8(2):265–85.

46. Caminade A, Ouali A. The dendritic effect illustrated with phosphorus dendrimers. Chem Soc Rev. 2014;44(12):3890–9.

47. Marcinkowska M, Janaszewska A, Lazniewska J, Trzepi P. Cytotoxicity of Dendrimers. Biomolecules. 2019;9(330):1–23.

48. Starpharma VivaGel [Internet]. Available from: https://www.starpharma.com/vivagel

49. Castro RI, Forero-doria O, Guzmán L. Perspectives of Dendrimer-based Nanoparticles in Cancer Therapy. Ann Brazilian Acad Sci. 2018;90(2):2331–46.

50. Hashemi M, Meghdad S, Parhiz H, Milanizadeh S, Amel S, Abnous K, et al. Gene delivery efficiency and cytotoxicity of heterocyclic amine-modified PAMAM and PPI dendrimers. Mater Sci Eng C. 2016;61:791–800.

51. Shao N, Su Y, Zhang H, Cheng Y. Comparison of generation 3 polyamidoamine dendrimer and generation 4 polypropylenimine dendrimer on drug loading , complex structure , release behavior , and cytotoxicity. Int J Nanomedicine. 2011;6:3361–72.

52. Kaur D, Jain K, Kumar N. A review on comparative study of PPI and PAMAM dendrimers. J Nanoparticle Res. Springer Netherlands; 2016;18(6):1–14.

53. Svenson S. Dendrimers as versatile platform in drug delivery applications. Eur J Pharm Biopharm. Elsevier B.V.; 2009;71(3):445–62.

54. Apalla Z, Lallas A, Sotiriou E, Lazaridou E, Ioannides D. Epidemiological trends in skin cancer. Dermatol Pract Concept. 2017;7(2):1–6.

55. Caekelbergh K, Leroy B, Saint-luc CU, Verhaeghe E. Photodynamic Therapy Using Methyl Aminolevulinate in the Management of Primary Superficial Basal Cell Carcinoma: Clinical and Health Economic Outcomes. J Drugs Dermatology. 2009;992(11):992–6.

56. Caekelbergh K, Annemans L, Lambert J, Roelandts R. Economic evaluation of methyl aminolaevulinate-based photodynamic therapy in the management of actinic keratosis and basal cell carcinoma. Photobiology. 2006;155(4):784–90.

57. Dabrzalska M, Zablocka M, Mignani S, Pierre J, Klajnert-maculewicz B. Phosphorus dendrimers and photodynamic therapy. Spectroscopic studies on two dendrimer-photosensitizer complexes : Cationic phosphorus dendrimer with rose bengal and anionic phosphorus dendrimer with methylene blue. Int J Pharm. 2015;492(1–2):266–74.

58. Dabrzalska M, Janaszewska A, Zablocka M, Mignani S, Majoral JP, Klajnert-maculewicz B. Complexing Methylene Blue with Phosphorus Dendrimers to Increase Photodynamic Activity. Molecules. 2017;22(345):1–13.

59. Vanerio N, Stijnen M, Mol BAJM De, Kock LM. Biomedical Applications of Photo- and Sono-Activated Rose Bengal: A Review. Photobiomodulation. 2019;37(7):383–94.

60. Nakonechny F, Barel M, David A, Koretz S, Litvak B, Ragozin E, et al. Dark Antibacterial Activity of Rose Bengal. Int J Mol Sci. 2019;20(3196).

61. Begley C, Ca B, Chalmers R, Situ P, Nelson JD. Review and analysis of grading scales for ocular surface staining. Ocul Surf. 2019;17(1):208–20.

62. Tomalia DA, Rookmaker M. Polymer Data Handbook. New York: Oxford University Press; 2009.

63. Lin S, Loh H, Ting K-N, Zeenathul Allaudin. Reduction of MTT to purple formazan by vitamin E isomers in the absence of cells. Trop Life Sci Res. 2015;26(1):111–20.

64. Sci JCI, Wang D, Imae T, Miki M. Fluorescence emission from PAMAM and PPI dendrimers. J Colloid Interface Sci. 2007;306(2):222–7.

65. Janaszewska A, Studzian M, Petersen JF, Ficker M, Paolucci V, Christensen JB, et al. Modified PAMAM dendrimer with 4-carbomethoxypyrrolidone surface groups-its uptake, efflux, and location in a cell. Colloids Surfaces B Biointerfaces. 2017;159:211–6.

66. Foroozandeh P, Aziz AA. Insight into Cellular Uptake and Intracellular Trafficking of Nanoparticles. Nanoscale Res Lett. Nanoscale Research Letters; 2018;13(1):1–12.

67. Chen L, Mccrate J, Lee J, Li H. The role of surface charge on the uptake and biocompatibility of hydroxyapatite nanoparticles with osteoblast cells. Nanotechnology. 2012;22(10):1–20.

68. Amaral M, Martins AS, Catarino J, Faísca P, Kumar P. How Can Biomolecules Improve Mucoadhesion of Oral Insulin ? A Comprehensive Insight using Ex-Vivo , In Silico , and In Vivo Models. Biomolecules. 2020;10(675):1–21.

69. Huo Q, Zhu J, Liu Y. pH-triggered surface charge-switchable polymer micelles for the co-delivery of paclitaxel/disulfiram and overcoming multidrug resistance in cancer. Int

J Nanomedicine. 2017;12:8631–47.

70. Hodgkinson N, Kruger CA, Abrahamse H. Targeted photodynamic therapy as potential treatment modality for the eradication of colon cancer and colon cancer stem cells. Tumor Biol. 2017;39(10):1–17.

71. Morton C, Nagore E, Ulrich C, Marmol VDEL, Peris K, Basset-seguin N. Update of the European guidelines for basal cell carcinoma management. Eur Dermatology Forum. 2014;24(3):312–29.

72. Dabrzalska M, Janaszewska A, Zablocka M, Mignani S, Majoral JP, Klajnert-maculewicz B. Cationic Phosphorus Dendrimer Enhances Photodynamic Activity of Rose Bengal against Basal Cell Carcinoma Cell Lines. Mol Pharm. 2017;14(5):1821–30.

73. Dabrzalska M, Benseny-cases N, Barnadas-rodríguez R, Mignani S, Zablocka M, Majoral J, et al. Fourier transform infrared spectroscopy (FTIR) characterization of the interaction of anti-cancer photosensitizers with dendrimers. Anal Bioanal Chem. 2015;408(2):535–544.

74. Klajnert B, Bryszewska M. Interactions between PAMAM dendrimers and gallic acid molecules studied by spectrofluorimetric methods. Bioelectrochemistry. 2007;70(1):50–2.

75. Clement S, Sobhan M, Deng W, Camilleri E, Goldys EM. Nanoparticle-mediated singlet oxygen generation from photosensitizers. J Photochem Photobiol. Elsevier B.V.; 2017;332:66–71.

76. Fini P, Castagnolo M, Catucci L, Cosma P, Agostiano A. Inclusion complexes of Rose Bengal and cyclodextrins. Thermochim Acta. 2004;418:33–8.

77. Klajnert B, Bryszewska M. The interaction of tryptophan and ANS with PAMAM dendrimers. Cell Mol Biol Lett. 2002;7(4):1087–94.

78. Cranfill PJ, Sell BR, Baird MA, Allen JR, Gruiter HM De, Kremers G, et al. Quantitative Assessment of Fluorescent Proteins. Nat Methods. 2016;13(7):557–62.

79. Rouhollah K, Pelin M, Serap Y, Gozde U, Ufuk G. Doxorubicin Loading, Release, and Stability of Polyamidoamine Dendrimer-Coated Magnetic Nanoparticles. J Pharm Sci.

2013;102(6):1825–35.

80. Zhang B, Yu H, Schlu AD, Halperin A, Kro M. Synthetic regimes due to packing constraints in dendritic molecules confirmed by labelling experiments. Nat Commun. 2013;4:1–9.

81. Wusiman A, Gu P, Wang D, Huang X. Cationic polymer modified PLGA nanoparticles encapsulating Alhagi honey polysaccharides as a vaccine delivery system for ovalbumin to improve immune responses. Int J Nanomedicine. 2019;14:3221–34.

82. Fröhlich E. The role of surface charge in cellular uptake and cytotoxicity of medical nanoparticles. Inernational J Nanomedicine. 2012;7:5577–91.

83. Entradas T, Waldron S, Volk M. The detection sensitivity of commonly used singlet oxygen probes in aqueous environments. J Photochem Photobiol. Elsevier; 2020;204(1):1011–344.

84. Kojima C, Toi Y, Harada A, Kono K. Preparation of Poly (ethylene glycol) - Attached Dendrimers Encapsulating Photosensitizers for Application to Photodynamic Therapy. Bioconjug Chem. 2007;18(3):663–70.

85. Kavyani S, Amjad-iranagh S, Modarress H. Aqueous Poly(amidoamine) Dendrimer G3 and G4 Generations with Several Interior Cores at pHs 5 and 7: A Molecular Dynamics Simulation Study. J Phys Chem. 2014;118(12):3257–66.

86. Klajnert B, Bryszewska M. Dendrimers: properties and applications. Acta Biochim Pol. 2001;48(1):199–208.

87. Estevão BM. Rose Bengal incorporated in mesostructured silica nanoparticles: structural characterization, theoretical modeling and siglet oxygen delivery. Phys Chem Chem Phys. 2015;17(40):26804–12.

88. Nishida M, Horiuchi H, Momotake A, Nishimura Y. Singlet molecular oxygen generation by water-soluble phthalocyanine dendrimers with different aggregation behavior. J Porphyr Phthalocyanines. 2011;15(1):47–53.

89. P-l S, Aw L, Daniallinia N, Jl H, Ma F, So P, et al. Long-term establishment, characterization and manipulation of cell lines from mouse basal cell carcinoma tumors. Exp Dermatol. 2006;15(9):742–50.

90. Jain K, Kesharwani P, Gupta U, Jain NK. Dendrimer toxicity : Let's meet the challenge. Int J Pharm. .; 2010;394(1–2):122–42.

91. Kumar S, Meena VK, Hazari PP, Sharma SK, Sharma RK. Rose Bengal attached and dextran coated gadolinium oxide nanoparticles for potential diagnostic imaging applications. Eur J Pharm Sci. 2018;117:362–70.

92. Karthikeyan K, Babu A. Enhanced photodynamic efficacy and efficient delivery of Rose Bengal using nanostructured poly(amidoamine) dendrimers: potential application in photodynamic therapy of cancer. Cancer Nanotechnol. 2011;2((1-6)):95–103.

93. Shrestha A, Hamblin MR, Kishen A. Characterization of a Conjugate between Rose Bengal and Chitosan for Targeted Antibiofilm and Tissue Stabilization Effects as a Potential. Antimicrob Agents Chemother. 2012;56(9):4876–84.

94. Chaudhuri S, Sardar S, Bagchi D, Dutta S. Photoinduced Dynamics and Toxicity of a Cancer Drug in Proximity of Inorganic Nanoparticles under Visible Light. ChemPhysChem. 2016;17(2):270–7.

95. International Organization for Standardization. ISO 10993-5:2009 Biological Evaluation of Medical Devices. Part 5: Tests for In Vitro Cytotoxicity. Geneva, Switzerland; 2009.

96. López-Garcia J, Lehocky M, Saha P. HaCaT Keratinocytes Response on Antimicrobial Atelocollagen Substrates : Extent of Cytotoxicity , Cell Viability and Proliferation. J Funct Biomater. 2014;5(2):43–57.